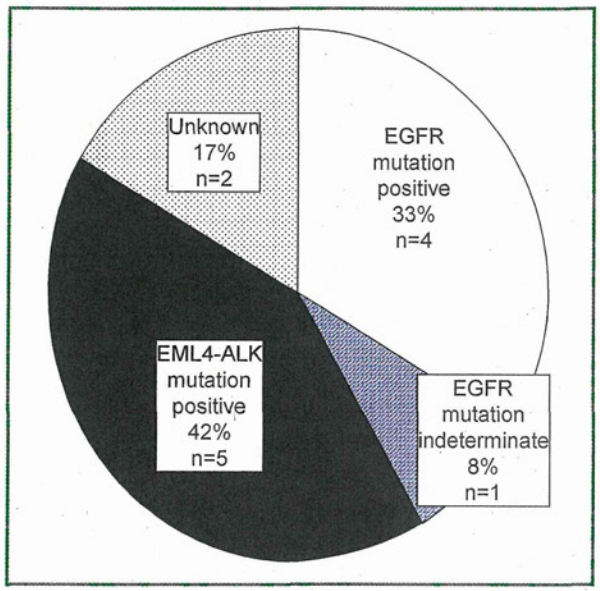

Figure 1. Frequency of gene abnormalities in 12 young patients with lung cancer aged 40 or younger.

The *EML4-ALK* fusion gene is recognized to be associated with the onset of lung cancer in young patients. *EML4-ALK* fusion gene has an exclusive relation with *EGFR* mutation and *K-ras* mutation (13). The frequency for the *EML4-ALK* fusion gene in this study was markedly higher than previous studies. Our sample-size was small, but gene abnormalities were identified in 75% in patients aged 40 and younger with lung cancer. Although all patients with *EGFR* activating mutation were treated with an *EGFR*-TKI, the overall survival was unsatisfactory. Unfortunately, we did not perform a re-examination for the gene abnormalities in the recurrent tumors. One of the potential mechanisms for short survival for these patients could be explained by the fact that 3 patients were heavy smokers, whose *k-ras* could be mutated. Moreover, we could evaluate only one case the *k-ras* status. Furthermore, the overall survival of the patients harboring the *EML4-ALK* fusion gene was also unsatisfactory, probably because *ALK*-TKI was not available at that time for these patients.

The results indicated that driver oncogenes were detected in 75% of our cases and that the frequency of *EML4-ALK* fusion gene was high in the young patients with non-small cell lung cancer. Our finding also suggests that the onset of non-small cell lung cancer in patients aged 40 or younger is more significantly related to gene abnormalities including driver oncogene mutation than to environmental factors.

Conclusions

In this study, we clarified that all 12 patients aged 40 and younger were non-small cell lung cancer and 9 in 12 patients

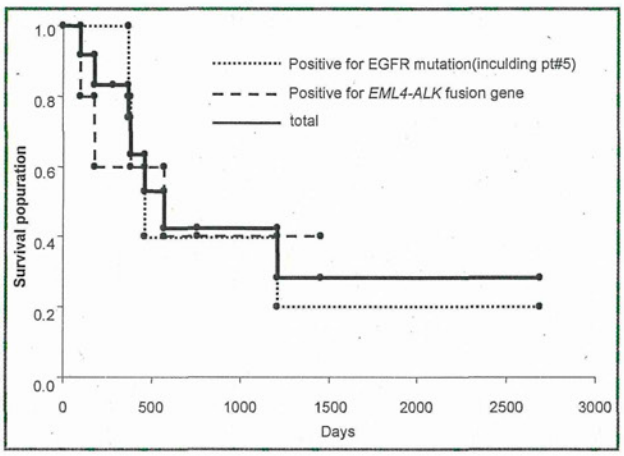

Figure 2. Survival curve of the patients.

were positive for the *EGFR* gene mutation or the *EML4-ALK* fusion gene. Our study revealed that ALK fusion gene affected carcinogenesis by the young patients in efficiency more than previous reports. Therefore, examination of gene abnormalities is especially important in young patients with lung cancer to provide a appropriate treatment modality.

Acknowledgements

We would like to thank Dr. Takeuchi, PhD, Pathology Project for Molecular Targets, the Cancer Institute, Japanese Foundation for Cancer Research, for detecting the *EML4-ALK* fusion gene by using the iAEP and FISH methods.

Disclosure: The authors declare no conflict of interest.

References

1. Jubelirer SJ, Wilson RA. Lung cancer in patients younger than 40 years of age. Cancer 1991;67:1436-8.
2. Larrieu AJ, Jamieson WR, Nelems JM, et al. Carcinoma of the lung in patients under 40 years of age. Am J Surg 1985;149:602-5.
3. Shepherd FA, Rodrigues Pereira J, Ciuleanu T, et al. Erlotinib in previously treated non-small-cell lung cancer. N Engl J Med 2005;353:123-32.
4. Mok TS, Wu YL, Thongprasert S, et al. Gefitinib or carboplatin-paclitaxel in pulmonary adenocarcinoma. N Engl J Med 2009;361:947-57.
5. Soda M, Choi YL, Enomoto M, et al. Identification of the transforming EML4-ALK fusion gene in non-small-cell lung cancer. Nature 2007;448:561-6.
6. Takeuchi K, Choi YL, Togashi Y, et al. KIF5B-ALK, a novel fusion oncokinase identified by an immunohistochemistry-based diagnostic system for ALK-positive lung cancer. Clin Cancer Res 2009;15:3143-9.
7. Mitsudomi T, Yatabe Y. Mutations of the epidermal growth factor receptor gene and related genes as determinants of epidermal growth factor receptor tyrosine kinase inhibitors sensitivity in lung cancer. Cancer Sci 2007;98:1817-24.

8. Toyooka S, Takano T, Kosaka T, et al. Epidermal growth factor receptor mutation, but not sex and smoking, is independently associated with favorable prognosis of gefitinib-treated patients with lung adenocarcinoma. Cancer Sci 2008;99:303-8.
9. Inamura K, Takeuchi K, Togashi Y, et al. EML4-ALK fusion is linked to histological characteristics in a subset of lung cancers. J Thorac Oncol 2008;3:13-7.
10. Takahashi T, Sonobe M, Kobayashi M, et al. Clinicopathologic features of non-small-cell lung cancer with EML4-ALK fusion gene. Ann Surg Oncol 2010;17:889-97.
11. Martelli MP, Sozzi G, Hernandez L, et al. EML4-ALK rearrangement in non-small cell lung cancer and non-tumor lung tissues. Am J Pathol 2009;174:661-70.
12. Paik JH, Choe G, Kim H, et al. Screening of anaplastic lymphoma kinase rearrangement by immunohistochemistry in non-small cell lung cancer: correlation with fluorescence in situ hybridization. J Thorac Oncol 2011;6:466-72.
13. Inamura K, Takeuchi K, Togashi Y, et al. EML4-ALK lung cancers are characterized by rare other mutations, a TTF-1 cell lineage, an acinar histology, and young onset. Mod Pathol 2009;22:508-15.

Cite this article as: Nagashima O, Ohashi R, Yoshioka Y, Inagaki A, Tajima M, Koinuma Y, Iwakami S, Iwase A, Sasaki S, Tominaga S, Takahashi K. High prevalence of gene abnormalities in young patients with lung cancer. J Thorac Dis 2013;5(1):27-30. DOI: 10.3978/j.issn.2072-1439.2012.12.02

Epilepsia, 53(3):558–564, 2012
doi: 10.1111/j.1528-1167.2011.03402.x

FULL-LENGTH ORIGINAL RESEARCH

Mutations of the *SCN1A* gene in acute encephalopathy

***Makiko Saitoh, *Mayu Shinohara, †Hideki Hoshino, †Masaya Kubota, ‡Kaoru Amemiya, §Jun-IchiTakanashi, ¶Su-Kyeong Hwang, ¶Shinichi Hirose, and *Masashi Mizuguchi**

*Department of Developmental Medical Sciences, Graduate School of Medicine, University of Tokyo, Tokyo, Japan; †Division of Neurology, National Center for Child Health and Development, Hachioji, Japan; ‡Department of Neurology, Tokyo Metropolitan Hachioji Children's Hospital, Tokyo, Japan; §Department of Pediatrics, Kameda Medical Center, Kamogawa, Japan; and ¶Department of Pediatrics and Research Institute for the Pathomechanisms of Epilepsy, Fukuoka University, Fukuoka, Japan

Summary

Purpose: Acute encephalopathy is the most serious complication of pediatric viral infections, such as influenza and exanthema subitum. It occurs worldwide, but is most prevalent in East Asia. Recently, there have been sporadic case reports of epilepsy/febrile seizure and acute encephalopathy with a neuronal sodium channel alpha 1 subunit (*SCN1A*) mutation. To determine whether *SCN1A* mutations are a predisposing factor of acute encephalopathy, we sought to identify *SCN1A* mutations in a large case series of acute encephalopathy including various syndromes.

Methods: We analyzed the *SCN1A* gene in 87 patients with acute encephalopathy, consisting of 20 with acute necrotizing encephalopathy (ANE), 61 with acute encephalopathy with biphasic seizures and late reduced diffusion (AESD), and six with nonspecific (unclassified) acute encephalopathy.

Key Findings: Three patients had distinct point mutations. Two of them had epileptic seizures prior to acute encephalopathy. Clinical and neuroradiologic findings of acute encephalopathy were diverse among the three patients, although all had a prolonged and generalized seizure at its onset. The first patient with V982L had partial epilepsy and AESD. The second patient with M1977L had febrile seizures and nonspecific acute encephalopathy. The third patient with R1575C had no seizures until the onset of ANE. M1977L was a novel mutation, whereas the remaining two, V982L and R1575C, have previously been reported in cases of Dravet syndrome and acute encephalopathy, respectively.

Significance: These findings provide further evidence that *SCN1A* mutations are a predisposing factor for the onset of various types of acute encephalopathy.

KEY WORDS: *SCN1A*, Ion channel gene defect, Acute encephalopathy status epilepticus, Seizure susceptibility.

Acute encephalopathy (AE) refers to brain dysfunction of acute onset that usually follows an infectious disease with fever. Pathologic substrate of AE is diffuse, noninflammatory brain edema. AE is most common in infants and young children, and is manifested clinically with stupor/coma and a febrile seizure, which is often severe and prolonged.

Based on clinical and neurologic findings, AE is classified into multiple syndromes, such as Reye's syndrome, acute necrotizing encephalopathy (ANE) (Mizuguchi et al., 1995), and acute encephalopathy with biphasic seizures and late reduced diffusion (AESD) (Takanashi et al., 2006). These syndromes show distinct computed tomography/magnetic resonance imaging (CT/MRI) features: diffuse brain edema in Reye's syndrome; bilateral, symmetric thalamic lesions in ANE; and cerebral cortical edema of subacute onset (usually appearing on the third to ninth day of illness, and sparing the perirolandic region) in AESD (Mizuguchi et al., 2007); however, about one-third of patients with AE show no such features and are unable to be classified into these syndromes (nonspecific AE). Pathogenesis of AE is complex, and much remains to be elucidated. The main pathomechanism differs among syndromes: metabolic disorder in Reye's syndrome, cytokine storm in ANE, and excitotoxicity in AESD (Mizuguchi et al., 2007). Delayed neuronal death after a severe/prolonged febrile seizure may play a major role in the pathophysiology of AESD (Mizuguchi et al., 2007; Takanashi et al., 2009).

Mutation of the neuronal sodium channel alpha 1 subunit (*SCN1A*) is the most common cause of hyperthermia-induced seizure susceptibility in patients with generalized epilepsy with febrile seizure plus (GEFS+) and Dravet syndrome (Escayg et al., 2000; Claes et al., 2001; Escayg et al., 2001; Wallace et al., 2001, 2003; Ohmori et al., 2002; Sugawara et al., 2002; Nabbout et al., 2003; Fukuma et al., 2004; Mantegazza et al., 2005; Escayg & Goldin, 2010). By contrast, *SCN1A* mutations are rare in febrile seizures other

Accepted December 20, 2011; Early View publication February 6, 2012.

Address correspondence to Dr. Makiko Saitoh, Department of Developmental Medical Sciences, Graduate School of Medicine, The University of Tokyo, 7-3-1 Hongo, Bunkyo, Tokyo 113-0033, Japan. E-mail: makisaito-tky@umin.net.jp

than GEFS+ and Dravet syndrome (Malacarne et al., 2002). Recently, there have been sporadic case reports of epilepsy/febrile seizure and AE with an *SCN1A* mutation (Sakakibara et al., 2009; Kobayashi et al., 2010; Takayanagi et al., 2010). In addition, children with Dravet syndrome occasionally have AE, which often causes death (Sakauchi et al., 2011). These cases suggest the role of *SCN1A* mutations in the pathogenesis of AE. To validate the hypothesis that *SCN1A* mutations are a predisposing factor of AE, we conducted *SCN1A* gene analysis in a large case series of AE, including various syndromes.

Methods

Patients

The Ethics Committees of the University of Tokyo approved this study. The parents or legal guardians of participants signed an informed consent form as approved by the ethics committees. Eighty-seven patients, 48 female and 39 male, who were diagnosed with AE and treated by 29 hospitals in Japan between September 2008 and August 2010, participated in this study. All the patients were of Japanese ethnicity. Diagnosis of AE was based on the following criteria: (1) impairment of consciousness showing acute onset, rapid progression and duration for more than 24 h, with or without seizures; (2) onset during the course of a febrile and/or infectious disease; and (3) exclusion of similar conditions, such as postictal stupor/coma, effect of anticonvulsants, meningitis, encephalitis, toxic encephalopathy, and metabolic errors. In addition, the patients were divided to three subgroups. Diagnosis of ANE and AESD was based on the criteria described previously (Hoshino et al., 2011). According to syndromic classification, 20 patients had ANE, 61 had AESD, and 6 had nonspecific AE (Table 1). There was no case of classical Reye's syndrome. Seven patients had preexisting febrile seizures and one patient had partial epilepsy before the onset of acute encephalopathy (Table 1). One hundred healthy adult Japanese volunteers without a history of AE served as control subjects.

Genetic analysis

Genomic DNA of patients with AE was prepared from ethylene diamine tetraacetic acid (EDTA)–treated whole blood samples using the QuickGene DNA whole blood kit (Fujifilm Corporation, Tokyo, Japan). *SCN1A* was screened by a direct sequencing method with an automatic sequencer, as described previously (Kobayashi et al., 2010). Reference sequence of mRNA was based on information available from GenBank (accession number: Human SCN1A. AF117907.1).

Results

Of the 87 AE cases studied, three had missense mutations—V982L, M1977L, and R1575C—none of which were found in the 100 controls. The *V982L* mutation was found in case 1 with partial epilepsy and AESD. The valine 982 residue is located on the transmembrane segment 6, domain II of SCN1A protein, is highly conserved among vertebrates, and shares homology with other types of sodium channels (Fig. 1). This mutation was previously reported in a patient with Dravet syndrome without myoclonic seizures and ataxia (Singh et al., 2009). The M1977L mutation was found in case 2 with GEFS+ and nonspecific AE. The methionine 1977 residue is located on near the

Table 1. Clinical data of 87 patients with acute encephalopathy (AE)

Diagnosis	Sex	Age at onset of AE (mean)	Family history of FS/epilepsy	Preexisting seizures	Preceding infection	Status epilepticus or cluster of seizures within 2 days after the onset of AE	Prognosis: Neurologic sequelae
ANE (n = 20)	Male 7 Female 13	8 months to 9 years 7 months (2 years 4 months)	FS 2 Epilepsy 0 None 18	FS 1 Epilepsy 0 None 19	HHV-6 3 Flu 4 RSV 2 Rota 1 NI 10	Yes 3 No 2 NA 15	Severe 9 Mild or none 9 NA 2
AESD (n = 61)	Male 28 Female 33	5 months to 6 years (1 year 9 months)	FS 6 Epilepsy 1 None 50 NA 4	FS 3 Epilepsy 1 None 53 NA 4	HHV-6 18 Flu 8 RSV 2 Others 4 NI 29	Yes 33 No 23 NA 5	Severe 14 Mild or none 41 NA 6
Nonspecific AE (n = 6)	Male 4 Female 2	1 year 9 months to 6 years 1 month (3 years 2 months)	FS 1 None 5	FS 3 None 3	Flu 2 NI 4	Yes 5 No 1	Severe 0 Mild or none 5 NA 1

Patients were classified into three syndromes: acute necrotizing encephalopathy (ANE), acute encephalopathy with biphasic seizures and late reduced diffusion (AESD), and nonspecific AE. FS, febrile seizures; NA, not available; HHV-6, human herpesvirus 6; Flu, influenza virus; RSV, respiratory syncytial virus; Rota, rotavirus; NI, not identified.

	1.V982L	2.M1977L	3.R1575C
SCN1A	VIGNLVVLNLF	KTDLTMSTAAC	TTILSRINLVF
CHIMPANZEE	----------	----------	----------
RAT	--R-------	----------	-S--------
MOUSE	----------	----------	-S--------
DROS	----------		
SCN2A	----------	---M-P--TSP	-N--YW-----
SCN3A	----------	---GSS--TSP	
SCN8A	----------		EN--YW-----

Figure 1.
Alignment of the amino acids surrounding the missense mutations in *SCN1A* of three acute encephalopathy cases. CHIMPANZEE (accession no. XP_515872), *Pan troglodytes* sodium channel α subunit; RAT (NP_110502), rat sodium channel α1 subunit; MOUSE (CAM17350), mouse sodium channel α1 subunit; DROS (NP_523371), *Drosophila melanogaster* sodium channel α subunit. *Drosophila* gene shares no homology with human *SCN1A* (BAC21101) at M1977 and R1575 locations. All other amino acid sequences are from human sodium channel α subunit expressed in the brain. SCN8A (NP_055006) shares no homology with SCN1A at the C-terminal end of the protein. Accession nos. of SCN2A and SCN3A are Q99250 and NP_008853.

C-terminus, and is conserved through mammalians (Fig. 1). The R1575C mutation was found in case 3 with ANE. This mutation has been reported previously in a patient with acute encephalitis with refractory, repetitive partial seizures (AERRPS) (Kobayashi et al., 2010), as well as in a patient with Rasmussen encephalitis with an autoantibody against the glutamate receptor GluR3 (Ohmori et al., 2008), and markedly alters the electrophysiologic properties of the sodium channel. The arginine 1575 residue is highly conserved among vertebrates (Fig. 1). The clinical course of these three patients is described briefly below.

Case 1: AESD with V982L mutation

This patient, a 2-year-old girl, was born small-for-date weighing 2,008 g, after gestation of 39 weeks. There was no family history of epilepsy or seizure disorders. From the age of 3 months, she had recurrent, afebrile complex partial seizures. There was no febrile seizure, myoclonic seizure, mental delay, or ataxia. The diagnosis of partial epilepsy was made, and prophylaxis with carbamazepine was begun. From 1 year and 11 months, she also had bronchial asthma. At 2 years and 3 months of age, she underwent treatment with intravenous theophylline for an asthma attack. She then had a respiratory infection with fever and vomiting, and developed myoclonic seizures, which evolved into prolonged generalized tonic convulsion. Status epilepticus was refractory to anticonvulsants and lasted 2 hours, requiring general anesthesia and mechanical ventilation. Although cranial CT was normal on day 2, coma persisted. Serum levels of aminotransferases and lactic dehydrogenase were very high. On day 5, she had clusters of partial seizures. CT revealed diffuse cerebral cortical edema. Based on the biphasic clinical course and serial CT findings, the diagnosis of AESD was made. She was treated with continuous infusion of thiopental (until day 21) and methylprednisolone pulse therapy. CT and MRI thereafter showed severe atrophy of the cerebral cortex with sparing of bilateral perirolandic regions (Fig. 2). She was eventually left with spastic quadriplegia and severe mental deficit.

Case 2: Nonspecific AE with M1977L mutation

This patient, a 3-year-old boy, was born uneventfully to nonconsanguineous parents. His uncle had had febrile convulsions during infancy. From the age of 1 year 6 months, he had recurrent febrile seizures. At 3 years of age, he had a respiratory infection with fever, and then had his sixth attack consisting of repeated generalized convulsions, six times during 24 h. Each convulsion lasted from several seconds to 5 min. Phenytoin (15 mg/kg) was given intravenously to prevent their recurrence. Consciousness disturbance (Glasgow Coma Scale score, E4V4M5) persisted for 24 h, and was explained neither by postictal stupor nor by sedative effects of phenytoin. Cranial CT revealed mild diffuse edema. Electroencephalography (EEG) on day 1 showed high-voltage slow activity in the right parietal area. He was diagnosed with nonspecific AE and recovered completely; however, he developed a cluster of afebrile seizures 1 month later. EEG showed bilateral frontal spike-waves. Valproate treatment successfully prevented seizures. He had neither mental delay nor ataxia.

Case 3: ANE with R1575C mutation

The patient is now a 12-year-old boy who was born uneventfully and showed normal development. At the age 9 months, he had acute gastroenteritis with fever (tempera-

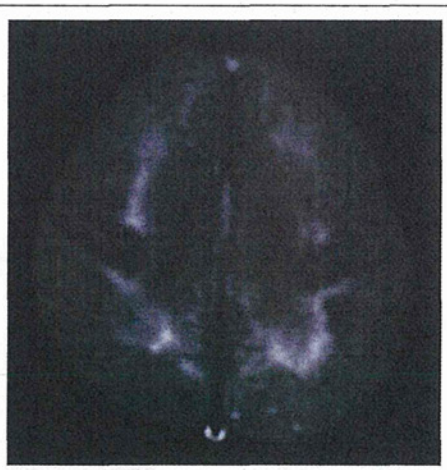

Figure 2.
Cranial MRI of a patient (case 1) with acute encephalopathy with biphasic seiaures and late reduced diffusion (AESD). Imaging at 4 years after AE (fluid-attenuated inversion recovery, FLAIR) showed cerebral atrophy, high signal intensity of the white matter, and sparing of the bilateral perirolandic regions.

ture 38°C) and diarrhea. Four days later, he was taken to hospital because of generalized seizure after several bouts of vomiting. On admission, he was afebrile and mentally obtunded, and had recurrent generalized tonic–clonic seizures. Blood examination showed slight elevation of C-reactive protein, and cerebrospinal fluid examination showed an increased protein level (370 mg/dl). MRI revealed abnormal signals in the bilateral thalamus and subcortical white matter on T_2-weighted images (Fig. 3A). Contrast T_1-weighted imaging showed medullary streaks in the white matter (Fig. 3B). Based on the clinical and imaging findings, the diagnosis of ANE was made. He was treated with intravenous anticonvulsants and gammaglobulin, and recovered without any sequelae. Two years later, his younger sister was also affected by ANE at the age of 8 months, and was eventually left with severe motor and cognitive impairment. She did not have the R1575C mutation.

Discussion

AE is a complex disorder in which multiple factors, both genetic and environmental, are involved. Environmental factors include not only infectious agents, such as influenza virus and human herpesvirus 6 (HHV-6), but also drugs, such as aspirin and theophylline (Mizuguchi et al., 2007). With regard to genetic factors, single nucleotide polymorphisms (SNPs) of carnitine transpalmitoyl transeferase II (*CPTII*) and Toll-like receptor 3 (*TLR-3*) have been identified as predisposing factors of AE (Chen et al., 2005; Hidaka et al., 2006; Shinohara et al., 2011). In our previous study on the *CPT II* gene, we found in two of the present cases (cases 2 and 3) thermolabile SNPs associated with susceptibility to AE (Shinohara et al., 2011). The relationship of these SNPs and AE is complex. For example, *CPTII* SNPs occur in association with two syndromes: AESD and ANE (Shinohara et al., 2011). For each syndrome, unidentified genes other than *CPTII* are likely to be also involved. On the other hand, there is one syndrome of AE caused by mutations of a single gene: *ANE1* (familial recurrent variant of ANE) due to mutation of the Ran-binding protein 2 (*RANBP2*) gene (Neilson et al., 2009).

In this study, we tested the possibility that mutation of another gene, *SCN1A*, is a genetic predisposition for the onset of AE. We performed *SCN1A* gene analysis in 87 Japanese patients with AE, and found point mutations, V982L, M1977L, and R1575C, in three (3.4%) of them. These results are comparable to those of a previous study, which found an *SCN1A* mutation in one of 15 AE patients (Kobayashi et al., 2010). Our study dealt with a large case series of AE, and found multiple patients with *SCN1A* mutations, thereby establishing the association between *SCN1A* mutations and AE.

In addition to our three patients, three additional patients with AE and a *SCN1A* mutation have been reported previously. Clinical and neuroradiologic findings of these six patients are variable (Table 2). With regard to epilepsy, two patients had Dravet syndrome, one had GEFS+, one had partial epilepsy, one had febrile seizures, and the remaining one had none. On the other hand, *SCN1A* missense mutations have been identified not only in patients with Dravet syndrome and GEFS+, but also in unaffected subjects without a seizure disorder (Ohmori et al., 2008). Therefore, their contribution to epilepsy and AE requires critical evaluation and further investigation.

With regard to AE, three had AESD, one had AERRPS, one had ANE, and one had nonspecific AE. Clinical features varied among the cases, although all had either prolonged seizures (status epilepticus; four cases) or a cluster of brief seizures (three cases), mostly with fever (five cases), on day 1 or 2, in contrast to mutation-negative patients in whom such seizures were absent in about 40% (Table 1). Prognosis also varied largely from severe psychomotor deficit to complete recovery. Notably, two patients with the same *SCN1A* mutation, R1575C, showed clinical phenotypes quite different from each other. Case 3 in this study had no

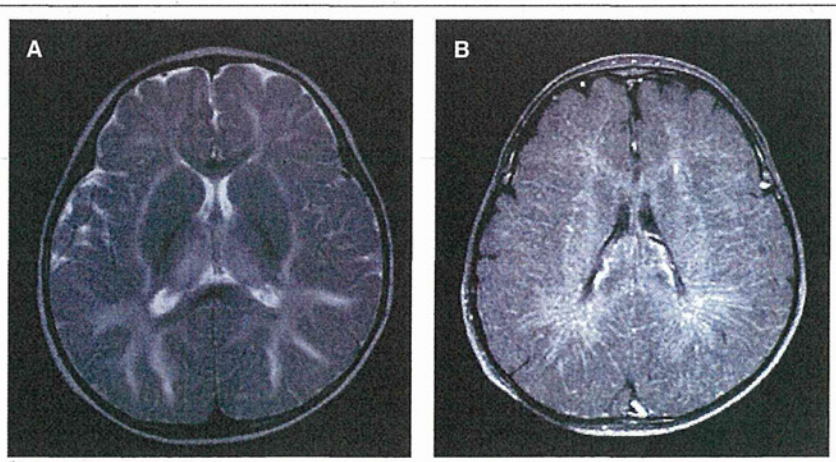

Figure 3.
Cranial MRI of a patient (case 3) with acute necrotizing encephalopathy (ANE). (**A**) T_2-weighted axial section shows high-intensity areas of bilateral thalami and the cerebral white matter. (**B**) Gadolinium-enhanced T_1-weighted axial image shows medullary streaks in the affected white matter lesions.

Epilepsia, 53(3):558–564, 2012
doi: 10.1111/j.1528-1167.2011.03402.x

Table 2. Characteristic of AE and preceding epilepsy in the [a]present (cases 1, 2 and 3) and previously reported cases

Case no.	Age	Gender	*SCN1A* mutation	Antecedent infection	Other etiologic factors	Precedimg epliIpsy or seizure dieorder	AE	Seizure at acute stage of AE	Neuroimaging findings	Prognosis	Reference
1[a]	2 years 3 months	F	V982L/ missense	Upper respiratory infection	Theophylline	Partial epilepsy	AESD	Status, febrile, on day1	CT/day 2, unremakable; CT/day 5, diffuse brain edema; follow-up MRI, central sparing	Spastic quadriplegia, severe MR	This study
2[a]	3 years	M	M1977L/ missense	Upper respiratory infection		GEFS+	Nonspecific AE	Cluster, febrile, on day1	CT/day 2, unremakable	Complete recovery	This study
3[a]	0 year 9 months	M	R1575C/ missense	Acute gastroenteritis	Family history of AE	None	Mimiking ANE	Cluster, afebrile, on day 1	MRI/day 2, bilateral thalamic lesions	Complete recovery	This study
4	1 year 4 months	F	R1892X/ nonsense	Rotavirus gastroenteritis		Dravet syndrome	AESD (HH)	Status, febrile, on day1	MR/day 6, left hemispheric edema	Mild MR (DQ = 71), right spastic heniplegia	Sakakibara et al., 2009
5	0 year 9 months	F	D43fs/ truncation	Fever of unknown etiology		Suspected Dravet syndrome	Atypical AESD	Status, febrile, on day1	MRI/day ×3, diffuse high signal intesity in cortex and subcortical white matter	Spastic quadriplegia, severe MR	Takayanagi et al., 2010
6	6 years 5 months	M	R1575C/ missense	Fever of unknown etiology		Febrile seizure	AERRPS	Cluster and status, febrile on day 2	CT and MRI, unremarkable	Mild MR	Kobayashi et al., 2010

Cases 4, 5, and 6 were reported in references.
GEFS+, generalized epilepsy with febrile seizure plus; AESD, acute encephalopathy with biphasic seizures and late reduced diffusion; AE, acute encephalopathy; ANE, acute necrotizing encephalopathy; HH, hemiconvulsion-hemiplegia syndrome; AERRPS, acute encephalitis with refractory, repetitive partial seizures.

epilepsy and ANE, whereas case 6 reported previously had febrile seizure and AERRPS (Kobayashi et al., 2010). This difference suggests the involvement of factors other than *SCN1A* mutation in the pathogenesis of AE.

The family history of case 3 deserves attention. The younger sister of this patient also had the same type of AE, despite the absence of *R1575C* mutation, which strongly suggests the involvement of another, as yet unidentified factor in this familial ANE. Comparison between the siblings revealed a longer duration of status epilepticus in the brother (case 3), and a worse prognosis in the sister. Plausibly, the *SCN1A* mutation contributed more to the evolution of status epilepticus, and the unidentified factor more to the development of bithalamic lesions and the overall neurologic damage.

In summary, we found *SCN1A* mutations in 3 of 87 cases of AE, and identified them as a predisposing genetic factor of AE. As for both epilepsy and AE, clinical phenotypes were variable among patients with *SCN1A* mutations. This variability, together with the family history of one patient (case 3), suggested that factors other than *SCN1A* mutations are also involved in the pathogenesis of AE.

Acknowledgments

Supported in part by a Grant-in-Aid for Scientific Research from the Japan Society for the Promotion of Science (No. 20390293, No. 22591176, 2149062, and 23659529), by a Grant-in-Aid for research (H23-Nanji-Ippan-78, 21B-5, 21210301, KB220001) from the Ministry of Health, Labour and Welfare, Japan, Adaptable and Seamless Technology Transfer Program through Target-driven R&D (A-STEP) Exploratory Research, Japan Science and Technology Agency (JST). The authors thank the members of the family for their cooperation in this study, and Akiyo Hamachi and Minako Yonetani (Department of Pediatrics and Research Institute for the Pathomechanisms of Epilepsy, Fukuoka University) for technical assistance.

Disclosures

None of author has any conflict of interest to disclosure.

We confirm that we have read the Journal's position on issues involved in ethical publication and affirm that this report is consistent with those guidelines.

References

Chen Y, Mizuguchi H, Yao D, Ide M, Kuroda Y, Shigematsu Y, Yamaguchi S, Yamaguchi M, Kinoshita M, Kido H. (2005) Thermolabile phenotype of carnitine palmitoyltransferase II variations as a predisposing factor for influenza-associated encephalopathy. *FEBS Lett* 579:2040–2044.

Claes L, Del-Favero J, Ceulemans B, Lage L, Van Broeckhoven C, De Jonghe P. (2001) De novo mutations in sodium-channel gene *SCN1A* cause severe myoclonic epilepsy in infancy. *Am J Hum Genet* 68:1327–1332.

Escayg A, Goldin AL. (2010) Sodium channel *SCN1A* and epilepsy: mutations and mechanisms. *Epilepsia* 51:1650–1658.

Escayg A, MacDonald BT, Meisler MH, Baulac S, Huberfeld G, An-Gourfinkel I, Brice A, LeGuern E, Moulard B, Chaigne D, Buresi C, Malafosse A. (2000) Mutations of *SCN1A*, encoding a neuronal sodium channel, in two families with GEFS+. *Nat Genet* 24:343–345.

Escayg A, Helis A, MacDonald BT, Haug K, Sander T, Meisler MH. (2001) A novel *SCN1A* mutation associated with generalized epilepsy with febrile plus-and prevalence of variants in patients with epilepsy. *Am J Hum Genet* 68:866–873.

Fukuma G, Oguni H, Shirasaka Y, Watanabe K, Miyajima T, Yasumoto S, Ohfu M, Inoue T, Watanachai A, Kira R, Matsuo M, Muranaka H, Sofue F, Zhang B, Kaneko S, Mitsudome A, Hirose S. (2004) Mutations of neuronl voltage-gated Na+ channel alpha I subunit gene *SCN1A* in core severe myoclonic epilepsy in infancy (SMEI) and in bordrline SMEI (SMEB). *Epilepsia* 45:140–148.

Hidaka F, Matsuo S, Muta T, Takeshige K, Mizukami T, Nunoi H. (2006) A missense mutation of the Toll-like receptor 3 gene in a patient with influenza-associated encephalopathy. *Clin Immunol* 119:188–194.

Hoshino A, Saitoh M, Oka A, Okumura A, Kubota M, Saito Y, Tkanashi J, Horose S, Yamagata T, Yamanouchi H, Mizuguchi M. (2011) Epidemiology of acute encephalopathy in Japan, with emphasis on the association of viruses and syndromes. *Brain Dev* doi: 10.1016/j.braindev.2011.07.012 [In press].

Kobayashi K, Ouchida M, Okumura A, Maegaki Y, Nishiyama I, Matsui H, Ohtsuka Y, Ohmori I. (2010) Genetic seizure susceptibility underlying acute encephalopathies in childhood. *Epilepsy Res* 91:143–152.

Malacarne M, Madia F, Gennaro E, Vaccca D, Guney AI, Buono S, Bernardina BD, Gaggero R, Gobbi G, Lispi ML, Malamaci D, Melideo G, Roccella M, Sferro C, Tiberti A, Vanadia F, Vigevano F, Viri F, Vitali MR, Bricarelli FD, Bianchi A, Zara F. (2002) Lack of SCN1A mutations in familial febrile seizures. *Epilepsia* 43:559–562.

Mantegazza M, Cambardella A, Rusconi R, Schiavon E, Annesi F, Cassulini RR, Labate A, Carrideo S, Chifari R, Canevini MP, Canger R, Franceschetti S, Annesi G, Wanke E, Quattrone A. (2005) Identification of an Nav1.1 sodium channel (*SCN1A*) loss-of-function mutation associated with familial simple febrile seizures. *Proc Natl Acad Sci U S A* 102:18177–18182.

Mizuguchi M, Abe J, Mikkaichi K, Noma S, Yoshida K, Yamanaka T, Kamoshita S. (1995) Acute necrotising encephalopathy of childhood: a new syndrome presenting with multifocal, symmetric brain lesions. *J Neurol Neurosurg Psychiatry* 58:555–561.

Mizuguchi M, Yamanouchi H, Ichiyama T, Shiomi M. (2007) Acute encephalopathy associated with influenza and other viral infections. *Acta Neurol Scand* 115:S45–S56.

Nabbout R, Gennaro E, Bernardina BD, Dulac O, Madia F, Bertini E, Capovilla G, Chiron C, Cristofori G, Elia M, Fontana E, Gaggero R, Granata T, Guerrini R, Loi M, La Selva L, Lispi ML, Matricardi A, Romeo A, Tzolas V, Valseriati D, Veggiotti P, Vigevano F, Vallee L, Dagna Bricarelli F, Bianchi A, Zara F. (2003) Spectrum of *SCN1A* mutations in severe myoclonic epilepsy of infancy. *Neurology* 60:1961–1967.

Neilson DE, Adams MD, Orr CM, Schelling DK, Eiben RM, Kerr DS, Anderson J, Bassuk AG, Bye AM, Childs AM, Clarke A, Crow YJ, Di Rocco M, Dohna-Schwake C, Dueckers G, Fasano AE, Gika AD, Gionnis D, Gorman MP, Grattan-Smith PJ, Hackenberg A, Kuster A, Lentschig MG, Lopez-Laso E, Marco EJ, Mastroyianni S, Perrier J, Schmitt-Mechelke T, Servidei S, Skardoutsou A, Uldall P, van der Knaap MS, Goglin KC, Tefft DL, Aubin C, de Jager P, Hafler D, Warman ML. (2009) Infection-triggered familial or recurrent cases of acute necrotizing encephalopathy caused by mutations in a component of the nuclear pore, RANBP2. *Am J Hum Genet* 84:44–51.

Ohmori I, Ouchda M, Ohtsuka Y, Oka E, Shimizu K. (2002) Significant correlation of the *SCN1A* mutations and severe myoclonic epilepsy in infancy. *Biochem Biophys Res Commun* 295:17–23.

Ohmori I, Ouchida M, Kobayashi K, Jitsumori Y, Inoue T, Shimizu K, Matsui H, Ohtsuka Y, Maegaki Y. (2008) Rasmussen encephalitis associated with *SCN1A* mutation. *Epilepsia* 49:521–526.

Sakakibara T, Nakagawa E, Saito Y, Sakuma H, Komaki H, Sugai K, Sasaki M, Kurahashi H, Hirose S. (2009) Hemiconvulsion-hemiplegia syndrome in a patient with severe myoclonic epilepsy in infancy. *Epilepsia* 50:2158–2162.

Sakauchi M, Oguni H, Kato I, Osawa M, Horose S, Kaneko S, Takahashi Y, Takayama R, Fujiwara T. (2011) Retrospective multiinstitutional study of the prevalence of early death in Dravet syndrome. *Epilepsia* 52:1144–1149.

Shinohara M, Saitoh M, Takanashi J, Yamanouchi H, Kubota M, Goto T, Kikuchi M, Shiihara T, Yamanaka G, Mizuguchi M. (2011) Carnitine palmitoyl transferase II polymorphism is associated with multiple syn-

dromes of acute encephalopathy with various viral infectious diseases. *Brain Dev* 33:512–517.

Singh NA, Pappas C, Dahle EJ, Claes LR, Pruess TH, De Jonghe P, Thompson J, Dixon M, Gurnett C, Peiffer A, White HS, Filloux F, Leppert MF. (2009) A role of *SCN9A* in human epilepsies, as a cause of febrile seizures and as a potential modifier of Dravet syndrome. *PLoS Genet* 5:e1000649.

Sugawara T, Mazaki-Miyazaki E, Fukushima K, Shimomura J, Fujiwara T, Hamano S, Inoue Y, Yamakawa K. (2002) Frequent mutations of *SCN1A* in severe myoclonic epilepsy in infancy. *Neurology* 58:1122–1124.

Takanashi J, Oba H, Barkovich AJ, Tada H, Tanabe Y, Yamanouchi H, Fujimoto S, Kato M, Kawatani M, Sudo A, Ozawa H, Okanishi T, Ishitobi M, Maegaki Y, Koyasu Y. (2006) Diffusion MRI abnormalities after prolonged febrile seizures with encephalopathy. *Neurology* 66:1304–1309.

Takanashi J, Tada H, Terada H, Barkovich AJ. (2009) Excitotoxicity in acute encephalopathy with biphasic seizures and late reduced diffusion. *Am J Neuroradiol* 30:132–135.

Takayanagi M, Haginoya K, Umehara N, Kitamura T, Numata Y, Wakusawa K, Hino-Fukuyo N, Mazaki E, Yamakawa K, Ohura T, Ohtake M. (2010) Acute encephalopathy with a truncation mutation in the *SCN1A* gene: a case report. *Epilepsia* 51:1886–1888.

Wallace RH, Scheffer IE, Barnet S. (2001) Neuronal sodium-channel α-subunit mutations in generalized epilepsy with febrile seizure plus. *Am J Hum Genet* 68:859–865.

Wallace RH, Hodgson BL, Grinton BE. (2003) Sodium channel α-subunit mutations in severe myoclonic epilepsy of infancy and infantile spasm. *Neurology* 61:765–769.

Journal of Virology

Oral Clarithromycin Enhances Airway Immunoglobulin A (IgA) Immunity through Induction of IgA Class Switching Recombination and B-Cell-Activating Factor of the Tumor Necrosis Factor Family Molecule on Mucosal Dendritic Cells in Mice Infected with Influenza A Virus

Etsuhisa Takahashi, Kosuke Kataoka, Irene L. Indalao, Keiko Konoha, Kazuyuki Fujii, Junji Chida, Dai Mizuno, Kohtaro Fujihashi and Hiroshi Kido

J. Virol. 2012, 86(20):10924. DOI: 10.1128/JVI.01207-12.
Published Ahead of Print 15 August 2012.

JVI
Journals.ASM.org

Oral Clarithromycin Enhances Airway Immunoglobulin A (IgA) Immunity through Induction of IgA Class Switching Recombination and B-Cell-Activating Factor of the Tumor Necrosis Factor Family Molecule on Mucosal Dendritic Cells in Mice Infected with Influenza A Virus

Etsuhisa Takahashi,[a] Kosuke Kataoka,[b] Irene L. Indalao,[a] Keiko Konoha,[a] Kazuyuki Fujii,[a] Junji Chida,[a] Dai Mizuno,[a] Kohtaro Fujihashi,[c] and Hiroshi Kido[a]

Division of Enzyme Chemistry, Institute for Enzyme Research,[a] and Department of Preventive Dentistry, Institute of Health Biosciences,[b] The University of Tokushima Graduate School, Tokushima, Japan, and Department of Pediatric Dentistry, Immunobiology Vaccine Center, Institute of Oral Health Research, University of Alabama at Birmingham, Birmingham, Alabama, USA[c]

We previously reported that the macrolide antibiotic clarithromycin (CAM) enhanced the mucosal immune response in pediatric influenza, particularly in children treated with the antiviral neuraminidase inhibitor oseltamivir (OSV) with low production of mucosal antiviral secretory IgA (S-IgA). The aims of the present study were to confirm the effects of CAM on S-IgA immune responses, by using influenza A virus (IAV) H1N1-infected mice treated with or without OSV, and to determine the molecular mechanisms responsible for the induction of mucosal IgA class switching recombination in IAV-infected CAM-treated mice. The anti-IAV S-IgA responses and expression levels of IgA class switching recombination-associated molecules were examined in bronchus-lymphoid tissues and spleens of infected mice. We also assessed neutralization activities of S-IgA against IAV. Data show that CAM enhanced anti-IAV S-IgA induction in the airway of infected mice and restored the attenuated antiviral S-IgA levels in OSV-treated mice to the levels in the vehicle-treated mice. The expression levels of B-cell-activating factor of the tumor necrosis factor family (BAFF) molecule on mucosal dendritic cells as well as those of activation-induced cytidine deaminase and Iμ-Cα transcripts on B cells were enhanced by CAM, compared with the levels without CAM treatment, but CAM had no effect on the expression of the BAFF receptor on B cells. Enhancement by CAM of neutralization activities of airway S-IgA against IAV *in vitro* and reinfected mice was observed. This study identifies that CAM enhances S-IgA production and neutralizing activities through the induction of IgA class switching recombination and upregulation of BAFF molecules in mucosal dendritic cells in IAV-infected mice.

Influenza brings repeating global threats to humans through annual epidemics, and there have been several pandemics, with considerable morbidity and mortality. In order to prevent complications and aggravation of the flu symptoms (25, 36), it is not uncommon, in Japan, to prescribe clarithromycin (CAM), a macrolide antibiotic developed by modification of erythromycin (11), combined with oseltamivir (OSV) as an antiviral neuraminidase inhibitor. In this regard, we have previously reported that administration of CAM in influenza A virus (IAV)-infected mice resulted in suppression of tumor necrosis factor alpha and augmentation of interleukin-12 production in the blood, resulting in alleviation of the flu symptoms (18), while oral treatment with OSV attenuated the induction of respiratory anti-IAV specific secretory IgA (S-IgA) immune responses (39). Furthermore, we have recently verified in IAV-infected children that oral CAM augmented the nasopharyngeal mucosal immune responses, while OSV suppressed the production of mucosal anti-IAV S-IgA (37). Of interest, we have also reported that 75% of patients treated with the combination of CAM and OSV showed increases in S-IgA production to levels similar to those seen in patients treated with CAM alone (37). Others have also reported that CAM acted on the viral replication cycles, resulting in inhibition of progeny virus production *in vitro* (25, 26), and modulated airway inflammation in IAV infection by reduction of the viral receptor, sialic acid with an α2,6 linkage on the airway epithelial cells, through inhibition of nuclear factor kappa B (NF-κB) expression and increase in intraendosomal pH (45). However, there is little information on the mechanisms of CAM-boosted induction of mucosal anti-IAV S-IgA.

Nasopharyngeal-associated lymphoreticular tissue and Peyer's patches are known as mucosal inductive sites where IgA-committed B cells undergo μ- to α-isotype class switching recombination (CSR). The IgA-committed B cells subsequently migrate to diffuse mucosal effector tissues, including the nasal passages (NPs) and intestinal lamina propria (iLP) (3, 22). In addition to these mucosal inductive tissues, T-cell-independent IgA CSR occurs in the iLP (8, 9, 12). Similarly, B cells of the isolated lymphoid follicles, scattered throughout the intestine, can undergo IgA CSR either from actual bacterial infection or from constant surveillance of commensals (10, 40). In this regard, both *in vitro* and *in vivo* studies have shown that B-cell-activating factor of the tumor necrosis factor family (BAFF) and the proliferation-inducing ligand

Received 14 May 2012 Accepted 6 August 2012
Published ahead of print 15 August 2012
Address correspondence or requests for reprints to Hiroshi Kido, kido@tokushima-u.ac.jp.

doi:10.1128/JVI.01207-12

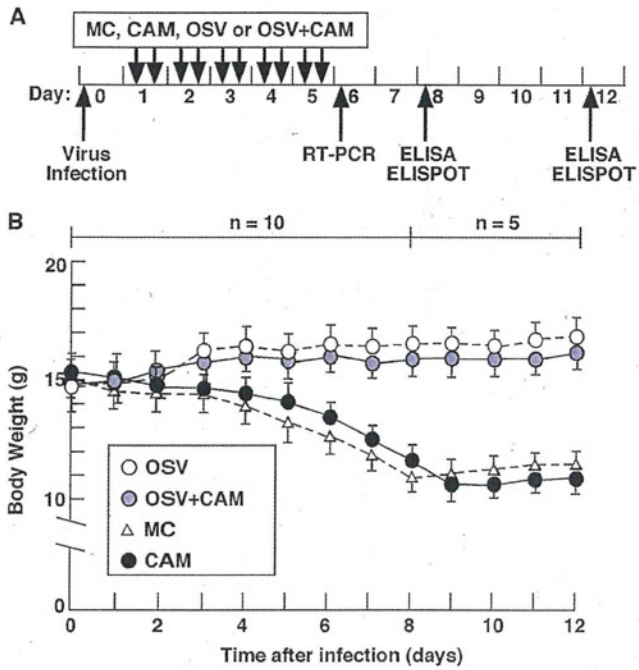

FIG 1 Experimental protocol for infection with IAV/PR8/34 virus. (A) At 20 h after infection with 25 PFU of IAV, mice were treated orally with 150 μg of CAM, 50 μg of OSV, OSV (50 μg) plus CAM (150 μg) in 100 μl of sterilized MC ($n = 10$), or 100 μl of MC as a control ($n = 10$). The dose was given twice daily for 5 days. (B) Changes in body weight in the four treatment groups. Data are means ± SEM (from day 0 to 7, $n = 10$; from day 8 to 12, $n = 5$).

(APRIL), members of the tumor necrosis factor ligand superfamily, promote T-cell-independent CSR of IgA via engagement of BAFF receptor (BAFF-R), transmembrane activator and calcium modulator cyclophilin ligand interactor (TACI), and B-cell maturation antigen (Ag) (BCMA) (4, 5, 24). In addition, BAFF and APRIL on dendritic cells (DCs) can induce the expression of activation-induced cytidine deaminase (AID) expression in murine B cells (24, 44). Recent studies have also reported that retinoic acid-producing DCs from mucosa-associated lymphoreticular tissue induce surface IgA and gut homing receptor expression on B cells in a T-cell-independent manner (17, 29). BAFF and APRIL on DCs interact with BAFF-R, BCMA, and TACI on B cells and induce IgA CSR (2).

The aims of the present study were to confirm the effects of CAM on S-IgA immune responses, by using IAV (H1N1)-infected weanling mice, and to determine the cellular and molecular mechanisms responsible for the induction of IgA CSR in IAV-infected mice treated with CAM.

MATERIALS AND METHODS

Animals and viral infection. All experiments were conducted in accordance with the animal care committee guidelines of Tokushima University. Specific-pathogen-free 4-week-old weanling BALB/c female mice were obtained from Japan SLC. The mice were nasally inoculated with 25 PFU of mouse-adapted IAV/PR8/34(H1N1) in 15 μl of saline under ketamine anesthesia at day 0. At 20 h after infection, the mice were divided into the following four groups and treated orally daily for 5 days (Fig. 1A): the CAM group ($n = 10$; 150 μg/head, every 12 h), the OSV group ($n = 10$, 50 μg/head, every 12 h), the CAM-OSV group ($n = 10$, CAM, 150 μg/head/12 h; OSV, 50 μg/head/12 h), and the vehicle–0.5% methylcellulose 400 (MC) group ($n = 10$, 100 μl of MC/head). OSV and CAM were dissolved in sterilized MC solution. The body weight was measured on the morning of each day after viral infection (Fig. 1B) (mean ± standard deviation [SD] at day 0, 14.9 ± 0.6 g).

For viral reinfection experiments, the mice were initially infected intranasally with 5 PFU of IAV/PR8/34(H1N1) in 15 μl of saline and then orally treated with OSV, CAM, OSV-CAM, and MC as described above for 5 days at 20 h after infection. Two weeks after the initial infection, the mice were infected again with 50× the 50% lethal dose (LD_{50}; 500 PFU) of IAV/PR8/34(H1N1) in saline instilled into the nostril. After infection, loss of body weight and survival of animals were monitored. The effects of the initial treatment of infected mice with OSV, CAM, OSV-CAM, and MC were analyzed at day 14 after reinfection. The mice were euthanized, and isolated lungs were fixed with 4% paraformaldehyde for histopathological evaluation as described previously (35).

Cell isolation from mucosal lymphoid tissues. At days 6, 8, and 12 after infection, mononuclear cells were isolated from mucosal lymphoid tissues (Fig. 1A). Mononuclear cells from the mediastinal lymph nodes (MeLNs) and spleen were isolated under aseptic conditions by the mechanical dissociation method as described previously (14, 17). Nasal passages (NPs) were isolated using a modification of the dissociation method described previously (14, 15, 17). Mononuclear cells were isolated from the lungs by a combination of an enzymatic dissociation procedure using collagenase type IV (0.5 mg/ml; Sigma-Aldrich, St. Louis, MO) followed by discontinuous Percoll (Amersham Biosciences, Piscataway, NJ) gradient centrifugation. To obtain B cells or DCs from the mucosal lymph nodes, mononuclear cells from the MeLNs, lungs, NPs, and spleen were incubated with anti-B220-conjugated or anti-CD11c-labeled microbeads (Miltenyi Biotec, Auburn, CA), based on the protocol supplied by the manufacturer (16) and were then positively selected with AutoMACS. The purified cell fraction consisted of >97% $B220^+$ or $CD11c^+$ cells, with >99% cell viability.

Analysis of mucosal immune responses to IAV by ELISA or ELISPOT assay. At days 8 and 12 after infection, nasal washes (NWs), bronchoalveolar fluids (BALF), and plasma were collected as described previously (27, 45) and subjected to enzyme-linked immunosorbent assay (ELISA) to determine anti IAV-specific S-IgA and IgG levels (27, 33, 39). Mononuclear cells isolated from the MeLNs, lungs, NPs, and spleen were subjected to an enzyme-linked immunosorbent spot (ELISPOT) assay to determine the numbers of IgA and IgG antibody (Ab)-forming cells (AFCs), as described previously (15, 17, 39).

Measurement of BAFF expression in BMDCs treated with or without CAM and poly(I·C). Bone-marrow-derived dendritic cells (BMDCs) from naïve mice were prepared as described previously (28). BMDCs were stimulated with CAM (15 μM) or poly(I·C) (Amersham Bioscience, Piscataway, NJ) (20 μg/ml) for 6 h at 37°C. A concentration of 15 μM CAM is the maximum serum concentration of CAM in clinical use (500 mg of oral administration) (13). The expression levels of BAFF were measured by quantitative reverse transcription (RT)-PCR (43).

RT-PCR and quantitative RT-PCR assays. Total RNAs were extracted from mononuclear cells isolated from the MeLNs, lung, NPs, spleen, and BMDCs. The proliferation-inducing ligand (AID; 349 bp), Iμ-Cα (267 bp), and glyceraldehyde-3-phosphate dehydrogenase (GAPDH; 355 bp) transcripts in mucosal B cells were amplified using specific primers as described previously (9, 20, 30, 34, 38). The following primers were used: AID, sense, 5′-GGCTGAGGTTAGGGTTCCATCTCAG-3′, and antisense, 5′-GAGGGAGTCAAGAAAGTCACGCTGGA-3′; Iμ-Cα, sense, 5′-CTCTGGCCTGCTTATTGTTG-3′, and antisense, 5′-GAGCTGGTG GGAGTGTCAGTG-3′; and GAPDH, sense 5′-CATCACCATCTTCCAG GA-3′, and antisense, 5′-GAGGGGCCATCCACAGTCTTC-3′. In order to examine the expression of BAFF and APRIL on mucosal DCs or their receptors on B cells, the cDNAs purified from DCs and B cells were amplified with a pair of specific primers for BAFF (285 bp), APRIL (597 bp), BAFF-R (521 bp), TACI (172 bp), and BCMA (167 bp) and by an RT-PCR method (16). The following primers were used:

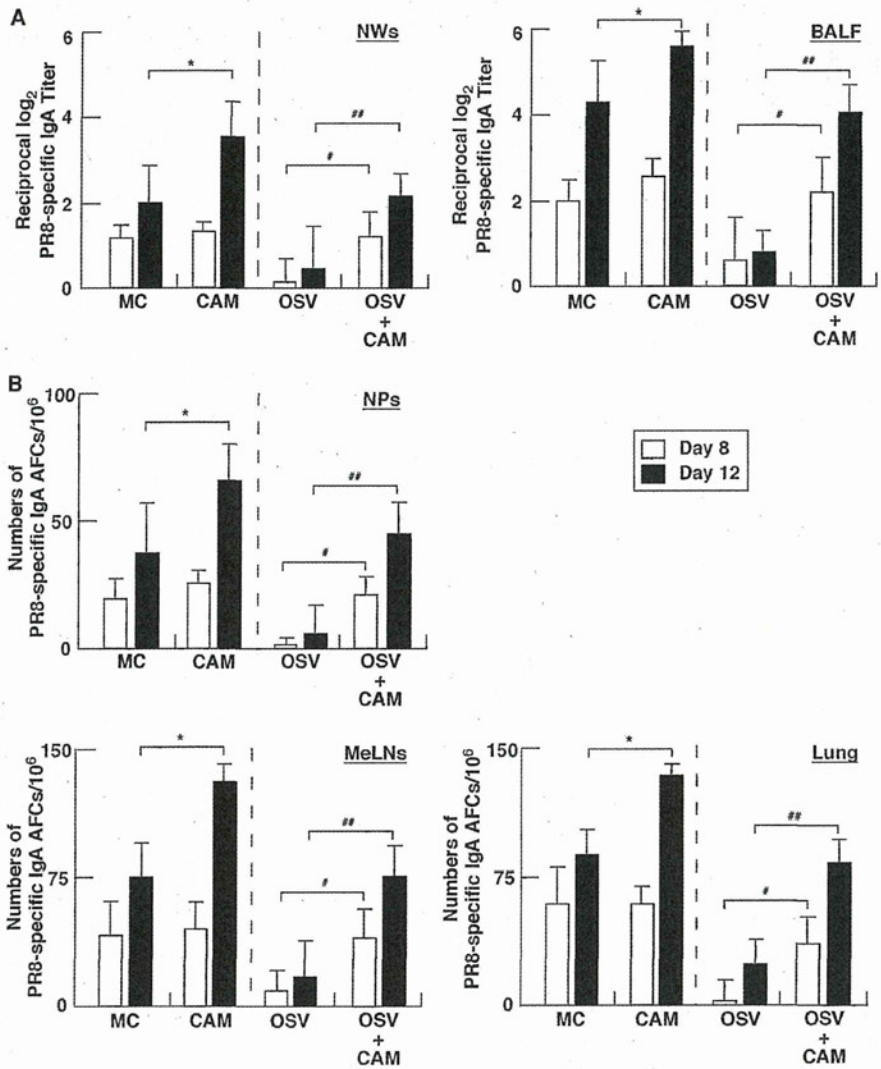

FIG 2 Anti-IAV-specific S-IgA immune response in external secretions and mucosal lymphoid tissues. Mice infected with IAV at day 0 were treated on five (from day 1 to 5) consecutive days with CAM, OSV, OSV-CAM, or MC. (A) At days 8 and 12, IAV-specific S-IgA levels were determined in nasal washings (NWs) and bronchoalveolar lavage fluid (BALF) by ELISA. Data are means ± SEM ($n = 5$). *, $P < 0.05$, versus MC; # and ##, $P < 0.05$ and $P < 0.01$, respectively, versus OSV. (B) At days 8 and 12, mononuclear cells isolated from the nasal passages (NPs), mediastinal lymph nodes (MeLNs), and lung were subjected to IAV-specific ELISPOT assay to determine the numbers of IgA AFCs. Data are means ± SEM ($n = 5$). *, $P < 0.05$ versus MC; # and ##, $P < 0.05$ and $P < 0.01$, respectively, versus OSV.

BAFF, sense, 5′-GAGAACAAAATAGTGGTGAGGCA-3′, and antisense, 5′-GTCGTCTCCGTTGCGTGAA-3′; APRIL, sense, 5′-ACCCTCCCTG CTACCTCTTGG-3′, and antisense, 5′-TCCTTCCCGAGATACCACCT G-3′; BAFF-R, sense, 5′-GACATGGGCGCCAGGAGACTCCGGGTCC GA-3′, and antisense, 5′-TGGGCCAGCTGTCTTGGTGGTCACCACCA GCTC-3′; TACI, sense, 5′-CCAGGATTGAGGCTAAGTAGCG-3′, and antisense, GGGGAGTTTGCTTGTGACC-3′; and BCMA, sense, 5′-CAA GCGTGACCAGTTCAGTGA-3′, and antisense, 5′-CGATCCGTCAAGC TGACCTG-3′.

Neutralizing activities for IAV. To assess IAV neutralization by mucosal S-IgA, Madin-Darby canine kidney (MDCK) cells were incubated with mixtures of IAV and S-IgA purified from NWs and BALF, as described previously (1). The S-IgA from NWs and BALF was purified with the Kaptiv-AE IgA affinity column according to the protocol provided by the manufacturer (Tecnogen S.p.A., Piacenza, Italy). Anti-influenza virus nucleoprotein monoclonal antibody (MAb) (QED Bioscience, San Diego, CA) and horseradish peroxidase-labeled anti-mouse IgG were used to detect the infected cells. The viral protein was visualized using the True-Blue peroxidase substrate (KPL, Inc., Gaithersburg, MD), and the numbers of cell foci/well were counted under a stereomicroscope.

Statistical analysis. The results are expressed as means ± 1 standard error of the mean (SEM). Data from the treatment groups were compared with those from the control, using an unpaired Mann-Whitney *U* test with Statview software (StatView 5.0 software (SAS Institute, Cary, NC). A *P* value of <0.05 was considered significant.

RESULTS

CAM significantly enhances airway S-IgA immune responses in the early stage of IAV infection, but not systemic IgG immune responses. After IAV infection, mice given OSV with or without CAM showed a slight but continuous increase in body weight during the 12-day experimental period (Fig. 1B). On the other hand, mice treated with CAM alone or MC as a control exhibited

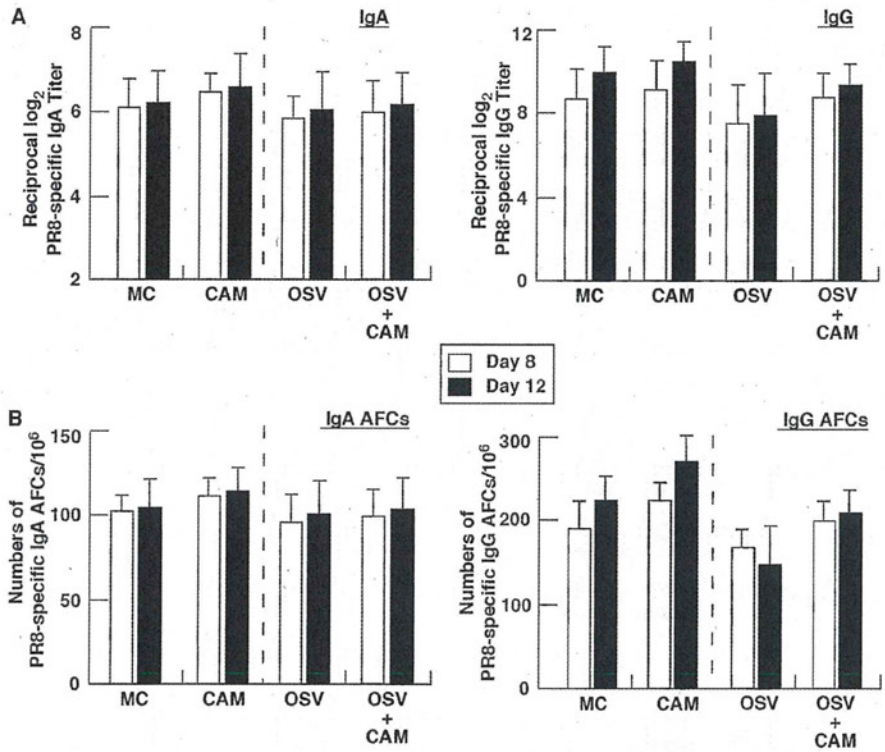

FIG 3 Systemic IAV-specific immune responses in mice after infection. Mice infected at day 0 were treated for five consecutive days (from days 1 to 5) with CAM, OSV, OSV-CAM, or MC. (A) IAV-specific IgA and IgG levels in plasma determined by ELISA. Data are means ± SEM ($n = 5$). There were no significant differences between CAM and MC and between OSV and OSV-CAM. (B) Mononuclear cells isolated from the spleen were subjected to the ELISPOT assay to determine the numbers of IgA and IgG AFCs. Data are means ± SEM ($n = 5$). There were no significant differences between CAM and MC and between OSV and OSV-CAM.

continuous loss of body weight from day 0 up to 26.7 to 27.4% loss at day 9 or 10 postinfection, followed by slow recovery (Fig. 1B). None of the mice died during the experimental period. These results suggest that OSV treatment for 5 days in the early stage of infection lessens the rate of complications and aggravation of flu symptoms in mice by suppression of viral replication.

To investigate the effect of the 5-day CAM treatment on antigen (Ag)-specific mucosal and systemic immune responses, we measured Ag-specific S-IgA levels in NWs and BALF as well as IgA and IgG levels in serum of mice at days 8 and 12 postinfection. CAM significantly increased anti-IAV-specific S-IgA levels in NWs and BALF of OSV-treated mice at days 8 and 12, compared with the levels in mice treated only with OSV (Fig. 2A). CAM also significantly increased S-IgA levels in NWs and BALF compared with the levels in MC-treated mice at day 12, the maximal phase of mucosal S-IgA induction (19, 37), although the effect was not significant at day 8, the intermediate phase (Fig. 2A). Furthermore, these findings were confirmed by Ag-specific ELISPOT assays. CAM significantly increased the numbers of Ag-specific IgA AFCs in respiratory effector tissues compared with MC and OSV treatment at day 8 and/or 12. On the other hand, there were no significant differences in the total numbers of S-IgA AFCs in these lymphoid tissues among the groups (data not shown). These results indicate that CAM upregulates Ag-specific S-IgA responses in mucosal effector tissues. However, CAM did not have a significant effect on the elevated levels of systemic Ag-specific IgA and IgG responses in serum of infected animals, compared with the control, such as MC or OSV treatment, although OSV treatment tended to suppress slightly the production of Ag-specific IgG and AFCs (Fig. 3A and B). Ag-specific Abs in airway secretions and serum at day 0 were below the detection levels. These experiments confirmed our previous findings of attenuated induction of antiviral S-IgA at days 8 and 12 in OSV-treated mice, compared with the vehicle-treated mice (39). Taken together, these findings indicate that CAM predominantly enhances mucosal immunity of both the attenuated antiviral S-IgA production in the OSV-treated mice and the S-IgA production in the MC-treated mice.

CAM induces IgA CSR in airway-associated lymphoid tissues. We next examined CSR from the μ- to α-chain in B cells from MeLNs, lung, NPs, and spleen (i.e., effector lymphoid tissues) of IAV-infected mice treated with CAM. The mRNA levels of AID and IμCα transcripts in mucosal B cells were analyzed by semiquantitative RT-PCR. Importantly, CAM significantly increased the levels of CSR-associated molecule-specific mRNAs in B cells from MeLNs, lung, and NPs, compared with the levels from MC- and OSV-treated mice, respectively (Fig. 4A), but had no such effect on in B cells from the spleen (Fig. 4B).

OSV significantly suppressed the expression levels of CSR-associated molecule-specific mRNAs in B cells from MeLNs, lung, and NPs, compared with the MC group (Fig. 4AA. In addition, OSV-CAM significantly increased the expression of AID- and IμCα-specific mRNAs in B cells from MeLNs, lung, and NPs compared with the OSV group (Fig. 4A). These results indicate that

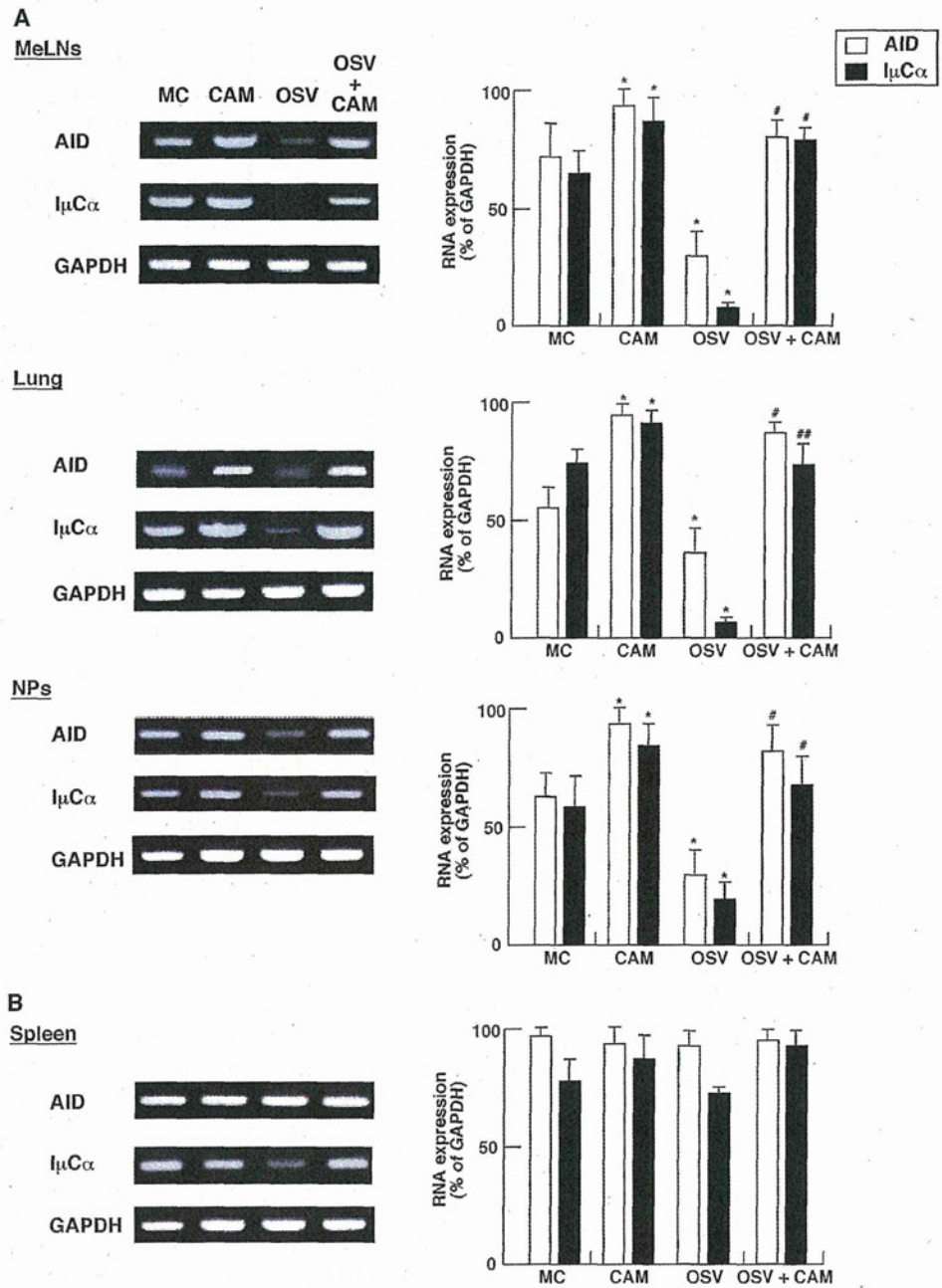

FIG 4 Preferential presence of AID, Iμ-Cα transcripts in B cells from the nasopharyngeal-tracheal effector sites in IAV-infected-mice treated with CAM, OSV, OSV-CAM, or MC. Total RNA extracted from the mediastinal lymph nodes (MeLNs), lung, nasal passages (NPs), and spleen of IAV-infected mice at day 6 was subjected to RT-PCR analysis. The left panels show representative results, and the graphs on the right show the expression level of the respective CSR-associated molecules relative to the density of GAPDH expression, calculated as 100 with ChemiDoc XRS Quantity One Analysis software (Bio-Rad). Data are means ± SEM from 5 mice for each group and represent a total of five separate experiments. *, $P < 0.05$ versus MC; # and ##, $P < 0.05$ and $P < 0.01$, respectively, versus OSV.

CAM predominantly enhances the recovery of reduced IgA CSR by OSV in mucosal effector tissues of IAV-infected mice.

CAM increases BAFF molecule expression on DCs from MeLNs, lung, and NPs, but not that of BAFF receptors on B cells. It is known that IgA CSR occurs through both a T-cell-dependent engagement with CD40-CD40 ligand and a T-cell-independent pathway (6, 12, 24). We have also shown that the APRIL molecule on oral-nasopharyngeal DCs mediates the T-cell-independent IgA CSR for innate immunity by interaction with the TACI molecule on B cells of mucosal effector tissues (16). In this regard, we next examined whether CAM induces the expression of BAFF and APRIL molecules on DCs from MeLNs, lung, and NPs at the early phase of IAV infection. Although the expression levels of BAFF and APRIL on DCs from MeLNs, lung, and NPs of IAV-infected OSV-treated mice were similar to those of the MC-treated mice, a significantly higher expression level of BAFF, but not APRIL, was

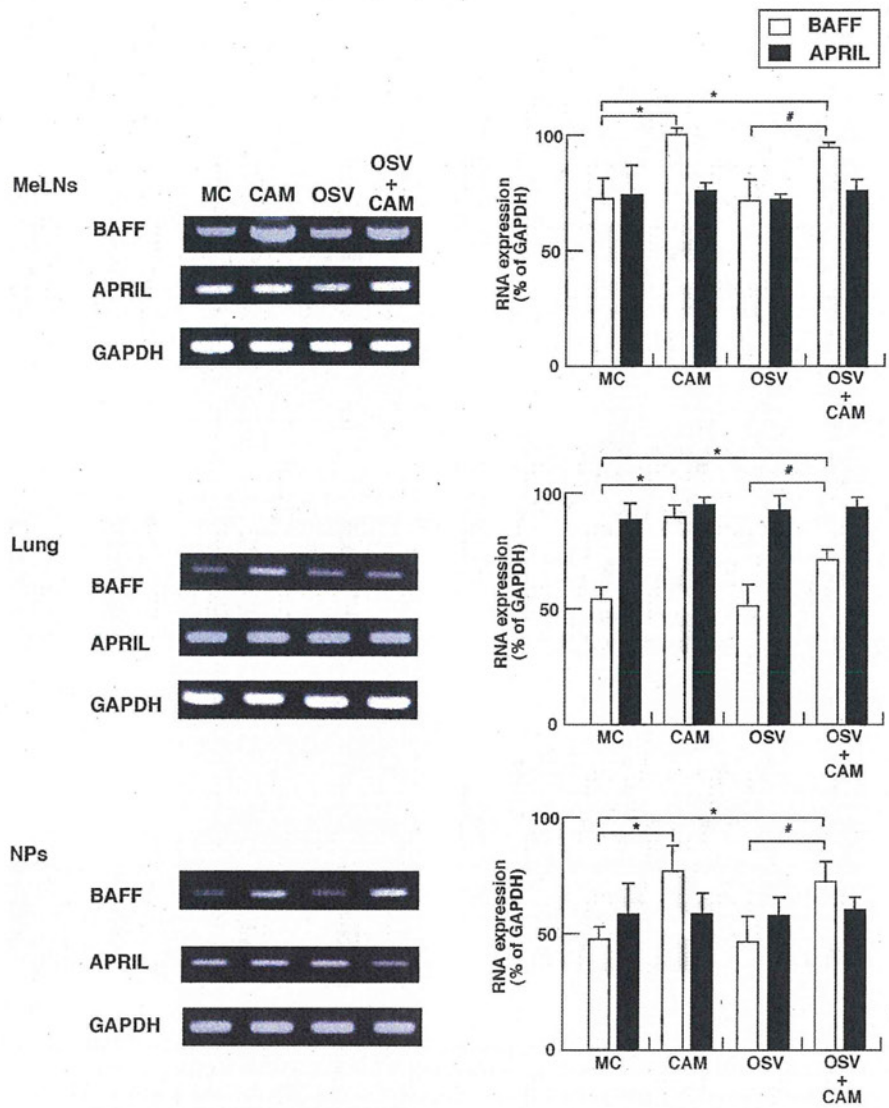

FIG 5 Expression of B-cell-activating factor (BAFF) and proliferation-inducing ligand (APRIL) in CD11c$^+$ DCs on mucosal effector sites. The day after the last dose of CAM, OSV, OSV-CAM, and MC (i.e., at day 6), mononuclear cells were isolated from the mediastinal lymph nodes (MeLNs), lung, and nasal passages (NPs) of IAV-infected mice, and mucosal DCs were purified with AutoMacs using anti-CD11c MAb-labeled microbeads, as described in Materials and Methods. Total RNA extracted from CD11C$^+$ DCs was subjected to RT-PCR analysis. The left panels show representative results, and the graphs on the right show the results of quantitative analysis. Data are means ± SEM from 5 mice for each group and represent a total of five separate experiments. *, $P < 0.05$ versus MC; #, $P < 0.05$ versus OSV.

noted on DCs from MeLNs, lung, and NPs of IAV-infected OSV-CAM-treated mice and CAM-treated mice compared with OSV- and MC-treated mice, respectively (Fig. 5).

We next analyzed by quantitative RT-PCR whether the effect of CAM on upregulation of BAFF on DCs is direct or indirect (Table 1). Although treatment of BMDCs with 20 μg/ml of poly(I·C) as a positive control (43) significantly increased BAFF expression on the cells, treatment with 15 μM CAM, the maximum serum concentration in clinical use (13), did not increase the expression. These results suggest that CAM indirectly enhances BAFF expression on DCs in the airway-associated lymphoid tissues and that BAFF-expressing mucosal DCs induce IgA CSR in the airway effector tissues.

TABLE 1 Quantitative RT-PCR analyses of BAFF expression in BMDCs

Treatment	Relative mRNA expression rate at[a]:	
	0 h	6 h
Vehicle (0.05% DMSO)[b]	0.30 ± 0.04	0.40 ± 0.16
CAM (15 μM)	0.25 ± 0.02	0.24 ± 0.07
Poly(I·C) (20 μg/ml)	0.30 ± 0.10	1.47 ± 0.37*

[a] After the cells had been treated with each reagent for 0 and 6 h, total RNA was isolated, and the expression levels of BAFF mRNA normalized to GAPDH mRNA were detected. Data are means ± SEM from four independent experiments. *, $P < 0.05$ versus vehicle at 6 h.

[b] DMSO, dimethyl sulfoxide.

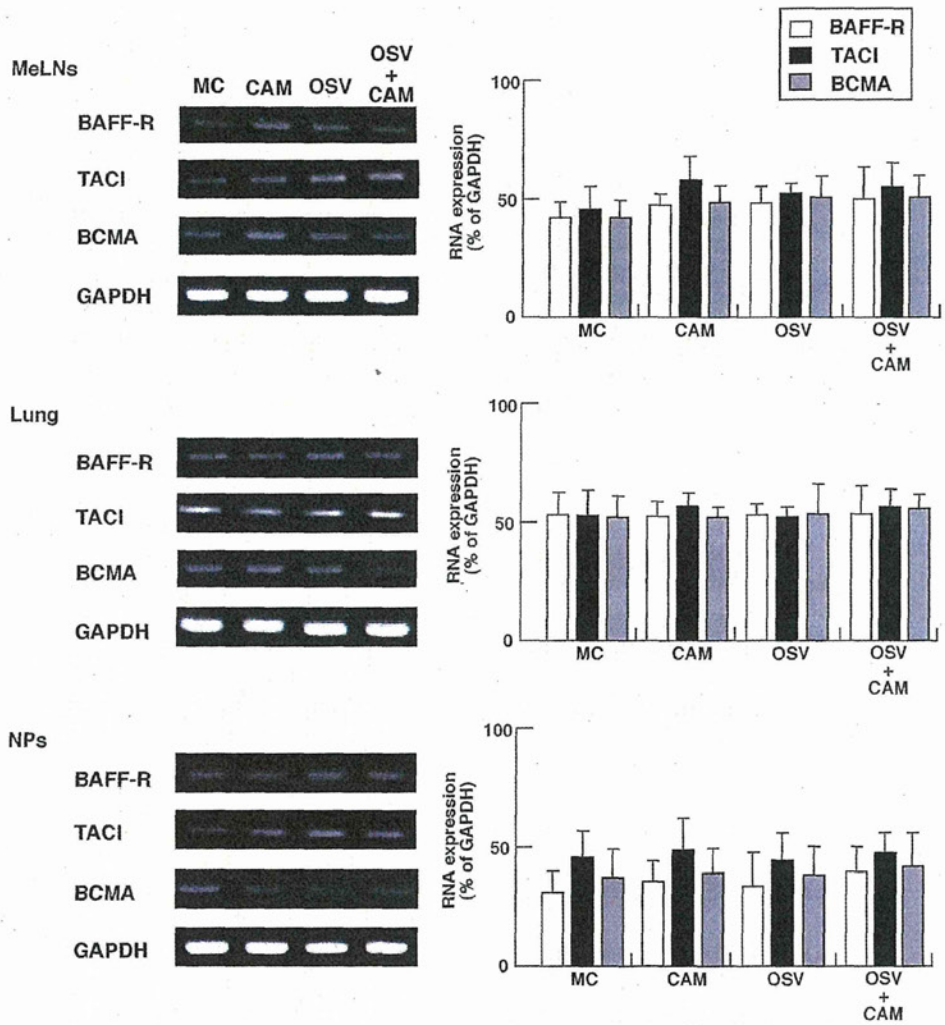

FIG 6 Expression of B-cell-activating factor (BAFF) and proliferation-inducing ligand (APRIL) receptor molecules (BAFF-R, transmembrane activator and calcium modulator cyclophilin ligand interactor [TACI], and B-cell maturation antigen [BCMA]) in mucosal B220$^+$ B cells. The day after the last dose of CAM, OSV, OSV-CAM, or MC, mononuclear cells were isolated from the mediastinal lymph nodes (MeLNs), lung, and nasal passages (NPs) of IAV-infected mice. The mucosal B cells were purified with AutoMacs using anti-B220 MAb-conjugated microbeads. Total RNA extracted from B220$^+$ B cells was subjected to RT-PCR analysis. The left panels show representative results, and the graphs on the right show the results of quantitative analysis. Data are means ± SEM of 5 mice for each group and represent a total of five separate experiments.

We also examined B cells from the MeLNs, lung, and NPs for their expression of BAFF-R, TACI, and BCMA, representing receptors for BAFF molecules on mucosal B cells. The results showed no significant change in the expression levels irrespective of the treatment (Fig. 6).

Reinforcement of anti-virus S-IgA by CAM exhibits neutralizing activities. Since mucosal S-IgA acts as a neutralizing Ab to pathogens and exotoxin, we determined *in vitro* the effects of treatment on the neutralizing activities of S-IgA. Incubation of MDCK cells with mixtures of IAV and S-IgA purified from NWs of the MC- and CAM-treated groups resulted in significant reductions in the numbers of infected-cell foci, compared with that from uninfected mice (Fig. 7, top). In contrast, similar *in vitro* experiments using S-IgA from the OSV-treated group showed significantly lower neutralizing activities than the MC- and CAM-treated groups. Even under the suppressed neutralizing activities in the OSV-treated mice, it is noted that additional combination of CAM with OSV significantly enhanced the neutralization activities of S-IgA fractions purified from BALF (Fig. 7, bottom). The combined treatment with CAM and OSV also tended to increase the neutralization activities of S-IgA fractions from NWs, but this was not significant (Fig. 7, top). These results indicate that CAM predominantly boosts mucosal S-IgA neutralization activities in BALF of IAV-infected OSV-treated mice.

We next confirmed reinforcement of protective immunity by CAM in reinfection experiments *in vivo* (Fig. 8). After initial IAV infection of mice followed by treatment with OSV, CAM, OSV-CAM, and MC for 5 days, the mice were reinfected with a lethal dose ($50\times$ LD_{50}; 500 PFU) of IAV at day 14 after the initial infection. All preinfected animals in the four treatment groups, such as the OSV group, the CAM group, the OSV-CAM group, and the MC group, survived with continuous increases in body weight (Fig. 8A). Although all mice ($n = 10$) in the four treatment groups showed resistance against a lethal dose of virus challenge, inflammatory cell mi-

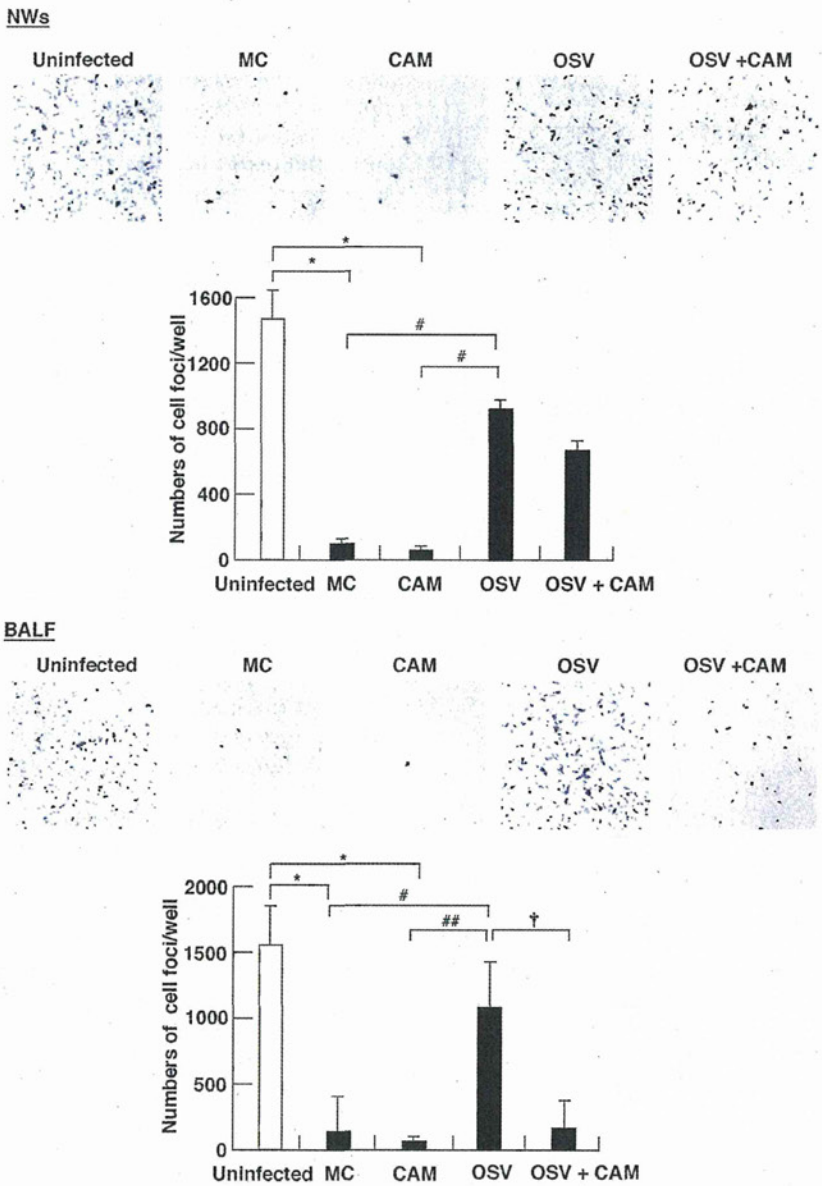

FIG 7 Neutralization activities of S-IgA in nasal washings (NWs) and bronchoalveolar lavage fluid (BALF) against IAV/PR8/34(H1N1) infection in MDCK cells. At day 12 postinfection, S-IgA was purified from NWs and BALF of mice treated with CAM, OSV, OSV-CAM, or MC or from naïve mice (uninfected), and 2 μg of purified S-IgA from each group was then preincubated with IAV (1,450 PFU, 100 μl) for 1 h at 37°C. Each mixture was subsequently incubated with confluent monolayers of MDCK cells at 37°C for 1 h for infection. Sixteen hours after infection, the cells were fixed with 4% paraformaldehyde–phosphate-buffered saline (PBS), permeabilized with 0.3% Triton X-100–PBS, and then visualized by TrueBlue peroxidase substrate. NWs and BALF from uninfected mice were used as the control. Original magnification, ×40. The values in the graph are mean numbers of infected cells ± SEM ($n = 4$). *, $P < 0.01$ versus uninfected; # and ##, $P < 0.05$ and $P < 0.01$, respectively, versus MC or CAM; †, $P < 0.05$ versus OSV-CAM.

gration in the lungs was most severe in the OSV-treated group at day 14 after reinfection (Fig. 8B). Lung inflammation was mild in the CAM-OSV-treated group, the CAM-treated group, and the MC-treated group compared with the lungs of noninfected mice.

DISCUSSION

Mucosal immunity works as the body's frontline of defense against invasion of pathogens. Against variant virus infections, mucosal S-IgA confers cross-protection, and thus may provide an overall higher protective activity than systemic IgG (23, 33). Furthermore, mucosal S-IgA is known as a noninflammatory Ab (21). Although heterosubtypic protection from influenza is not only mediated by cytotoxic T cells (31), mucosal S-IgA and respiratory B cells induced by nasal vaccination and natural infection (7, 32) are crucial in protecting against IAV infection. In addition, humoral and protective immunity associated with antihemagglutinin specific IgA elicited by primary infection or vaccination is important for the prevention of secondary infection with different virus subtypes (41). Therefore, we consider that induction of mucosal S-IgA is critical for immune protection against IAV infection.

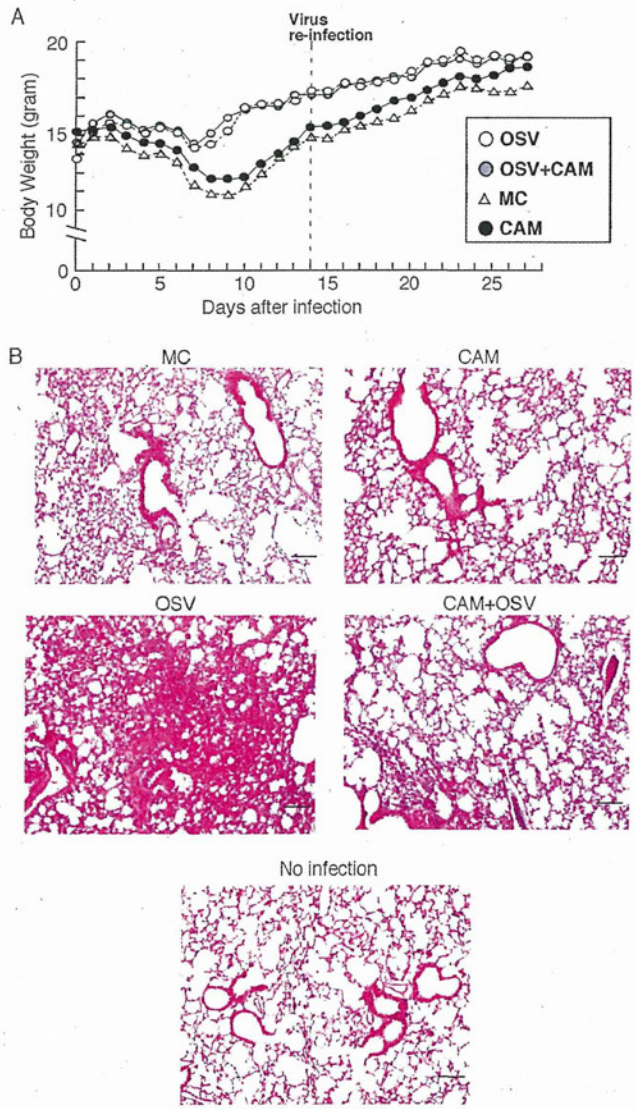

FIG 8 Reinforcement of protective immunity by CAM in reinfected mice. (A) At 20 h after infection with 5 PFU of IAV, mice were treated orally with CAM, OSV, OSV-CAM, or MC as described in the legend to Fig. 1. (A) Changes in body weight in the four treatment groups ($n = 10$). Data are means ± SEM. (B) Hematoxylin-and-eosin-staining sections in the lungs of four groups of mice at day 14 after reinfection and noninfection control mice. Each result is representative of 10 animals in each group. Bar, 100 μm.

In the present study, using the IAV-infected mice model, we demonstrated that CAM boosted the induction of sufficient mucosal S-IgA for protection against IAV infection in the respiratory tract (Fig. 2 and 7). As shown in the results in Fig. 2 and our recent animal (45) and human (3) studies, OSV treatment attenuated S-IgA production in the airway. In contrast, CAM enhanced respiratory S-IgA responses in OSV-treated mice and naïve mice. However, no significant differences were seen between the OSV- and OSV-CAM-treated mice with regard to the percentages of $CD11c^+$ DCs on NPs and MeLNs at day 6 (data not shown). The findings of reinforcement of neutralizing activities of S-IgA by CAM (Fig. 7) were supported by the results of reinfection experiments. The lung inflammation of IAV-infected OSV-CAM-treated mice was definitely mild in reinfection compared with that of IAV-infected OSV-treated mice (Fig. 8). These results support boosting of protective immunity by CAM in IAV-infected mice.

Previous studies indicated that AID is essential for CSR, which specifically occurs in activated B cells (4, 12, 24), and that Iμ-Cα transcript is a hallmark for active IgA CSR *in vivo* (20). To study the mechanisms of CAM-enhanced S-IgA production, we investigated the expression of AID and Iμ-Cα molecules involved in the induction of mucosal IgA CSR by B cells of the MeLNs, lung, and NPs. The results showed higher expression of AID and Iμ-Cα molecules in B cells from the mucosal lymph nodes in the CAM- and OSV-CAM-treated groups, but surprisingly low expression in the OSV-treated group, compared with the MC vehicle-treated group. These findings indicate that CAM induces T-cell-independent IgA CSR at the respiratory effector sites. In this regard, previous studies described a T-cell-independent IgA CSR pathway, in addition to the classical T-cell-dependent CSR in the intestinal mucosa (6), and we have also recently reported the upregulation of T-cell-independent μ- to α-isotype CSR on B-1 B cells of oral-nasopharyngeal effector tissues following the use of naïve cholera toxin as a nasal adjuvant, with T-cell-independent Ag (16). Furthermore, the present study showed that OSV inhibited the induction of T-cell-independent IgA CSR in respiratory effector sites, whereas OSV-CAM restored the suppressed induction. These findings suggest that the combination of CAM and OSV enhances anti-IAV S-IgA production, whereas OSV suppresses such processes.

It has been reported that both intestinal DCs and epithelial cells induce CD40-independent IgA CSR through BAFF and APRIL molecules (12, 24). In addition, we have also reported that APRIL-expressing DCs in oral-nasopharyngeal mucosal effector tissues induced IgA CSR on mucosal B-1 B cells following the use of naïve cholera toxin with T-cell-independent Ag as a nasal adjuvant (16). We also studied the cellular and molecular mechanisms of T-cell-independent IgA CSR in the MeLNs, lung, and NPs in CAM-treated mice by focusing on DCs from these mucosal lymph nodes of mice treated with CAM and their potential roles in the induction of T-cell-independent μ- to α-isotype CSR. The results showed that CAM increased the expression of BAFF molecules on DCs of the mucosal lymphoid tissues, compared with the other treatment groups (Fig. 5). However, CAM did not increase the expression of APRIL on DCs of the mucosal lymph nodes. These results suggest that BAFF-expressing DCs play a key role in IgA CSR by B cells in respiratory effector tissues. In this regard, a recent study reported that intestinal DCs activated through Toll-like receptor 5 signaling produce retinoic acid and induce IgA production by peritoneal B cells (42). Thus, it is possible that CAM stimulates virus-specific S-IgA responses through the production of retinoic acid by activated DCs in the MeLNs, lung, and NPs.

Although it is important to identify the receptors for the BAFF molecule on B cells that are responsible for the induction of IgA CSR, stable expression of BAFF-R, TACI, and BMCA molecules was noted on B cells from the MeLNs, lung, and NPs in IAV-infected mice treated with CAM, OSV, OSV-CAM, or MC, and no significant differences in BAFF-R, TACI, and BCMA expression were evident among these groups. Taken together, the results indicate that CAM stimulates DCs in the mucosal lymphoid tissues and plays an important role in IgA CSR by upregulation of expres-

sion of BAFF molecule. However, data in the experiments to clarify whether the effect of CAM on upregulation of BAFF on DCs is a direct or indirect effect suggest that CAM indirectly enhances BAFF expression on mucosal DCs (Table 1). Further screening studies for the target molecule(s) of CAM are currently in progress.

In summary, using IAV-infected weanling mice, the present study demonstrated that orally administered CAM enhances mucosal IAV-specific S-IgA immune responses and has neutralization activities. Thus, based on the production of mucosal S-IgA Ab, we consider that the combination of CAM-OSV treatment for IAV could potentially prevent complications and aggravation of the flu symptoms at an early stage of infection.

ACKNOWLEDGMENTS

We thank Rebekah S. Gilbert for editorial assistance, scientific discussion, and critiques during the preparation of the manuscript.

The authors declare they have no potential conflicts of interest.

Financial support for this work was provided by Grant-in-Aid 24249059 and Special Coordination Funds for the Promotion of Science and Technology from the Ministry of Education, Culture, Sports, and Science and Technology of Japan.

REFERENCES

1. **Al-Garawi AA, et al.** 2009. Acute, but not resolved, influenza A infection enhances susceptibility to house dust mite-induced allergic disease. J. Immunol. 182:3095–3104.
2. **Barone F, Patel P, Sanderson JD, Spencer J.** 2009. Gut-associated lymphoid tissue contains the molecular machinery to support T-cell-dependent and T-cell-independent class switch recombination. Mucosal Immunol. 2:495–503.
3. **Brandtzaeg P, Farstad IN, Haraldsen G.** 1999. Regional specialization in the mucosal immune system: primed cells do not always home along the same track. Immunol. Today 20:267–277.
4. **Castigli E, et al.** 2004. Impaired IgA class switching in APRIL-deficient mice. Proc. Natl. Acad. Sci. U. S. A. 101:3903–3908.
5. **Castigli E, et al.** 2005. TACI and BAFF-R mediate isotype switching in B cells. J. Exp. Med. 201:35–39.
6. **Cerutti A.** 2008. The regulation of IgA class switching. Nat. Rev. Immunol. 8:421–434.
7. **Choi YS, Baumgarth N.** 2008. Dual role for B-1a cells in immunity to influenza virus infection. J. Exp. Med. 205:3053–3064.
8. **Crouch EE, et al.** 2007. Regulation of AID expression in the immune response. J. Exp. Med. 04:1145–1156.
9. **Fagarasan S, Kinoshita K, Muramatsu M, Ikuta K, Honjo T.** 2001. *In situ* class switching and differentiation to IgA-producing cells in the gut lamina propria. Nature 413:639–643.
10. **Hamada H, et al.** 2002. Identification of multiple isolated lymphoid follicles on the antimesenteric wall of the mouse small intestine. J. Immunol. 168:57–64.
11. **Hashisaki GT.** 1995. Update on macrolide antibiotics. Am. J. Otolaryngol. 16:153–157.
12. **He B, et al.** 2007. Intestinal bacteria trigger T cell-independent immunoglobulin A2 class switching by inducing epithelial cell secretion of the cytokine APRIL. Immunity 26:812–826.
13. **Honeybourne D, Kees F, Andrews JM, Baldwin D, Wise R.** 1994. The levels of clarithromycin and its 14-hydroxy metabolite in the lung. Eur. Respir. J. 7:1275–1280.
14. **Kataoka K, et al.** 2011. Nasal dendritic cell targeting flt3 ligand as a safe adjuvant elicits effective protection against fatal pneumococcal pneumoniae. Infect. Immun. 79:2819–2828.
15. **Kataoka K, et al.** 2007. Nasal cholera toxin elicits IL-5 and IL-5 receptor alpha-chain expressing B-1a B cells for innate mucosal antibody responses. J. Immunol. 178:6058–6065.
16. **Kataoka K, et al.** 2011. Oral-nasopharyngeal dendritic cells mediate T cell-independent IgA class switching on B-1 B cells. PLoS One 6:e25396. doi:10.1371/journal.pone.0025396.
17. **Kataoka K, et al.** 2004. Nasal Flt3 ligand cDNA elicits CD11c+CD8+ dendritic cells for enhanced mucosal immunity. J. Immunol. 172:3612–3619.
18. **Kido H, Okumura Y, Yamada H, Le TQ, Yano M.** 2007. Protease essential for human influenza virus entry into cells and their inhibitors as potential therapeutic agents. Curr. Pharm. Des. 13:405–414.
19. **Kido H, et al.** 2011. Attenuation of respiratory immune responses by antiviral neuraminidase inhibitor treatment and boost of mucosal immunoglobulin A response by co-administration of immuno-modulator clarithromycin in pediatric influenza. Influenza Other Respir. Viruses 5:240–243.
20. **Kinoshita K, Harigai M, Fagarasan S, Muramatsu M, Honjyo T.** 2001. A hallmark of active class switch recombination: transcripts directed by I promoters on looped-out circular DNAs. Proc. Natl. Acad. Sci. U. S. A. 98:12620–12633.
21. **Kiyono H, Kunisawa J, McGhee JR, Mestecky J.** 2008. The mucosal immune system, p 983–1030. *In* Paul WE (ed), Fundamental immunology, 5th ed. Lippincott Williams & Wilkins, Philadelphia, PA.
22. **Kunkel EJ, Butcher EC.** 2003. Plasma-cell homing. Nat. Rev. Immunol. 3:822–829.
23. **Liew FY, Russel SM, Appleyard G, Brand CM, Beale J.** 1984. Cross-protection in mice infected with influenza A virus by the respiratory route is correlated with local IgA antibody rather than serum antibody or cytotoxic T cell reactivity. Eur. J. Immunol. 14:350–356.
24. **Litinskiy MB, et al.** 2002. DCs induce CD40-independent immunoglobulin class switching through BLyS and APRIL. Nat. Immunol. 3:822–829.
25. **Maeda S, Yamada Y, Nakamura H, Maeda T.** 1999. Efficacy of antibiotics against influenza-like illness in an influenza epidemic. Pediatr. Int. 41:274–276.
26. **Miyamoto D, et al.** 2008. Clarithromicin inhibits progeny virus production from human influenza virus-infected host cells. Biol. Pharm. Bull. 31:217–222.
27. **Mizuno D, Ide-Kurihara M, Ichinomiya T, Kubo I, Kido H.** 2006. Modified pulmonary surfactant is a potent adjuvant that stimulates the mucosal IgA production in response to the influenza virus antigen. J. Immunol. 176:1122–1130.
28. **Mizuno D, et al.** 2011. Surfactant protein C is an essential constituent for mucosal adjuvanticity of Surfacten, acting as an antigen delivery vehicle and inducing both local and systemic immunity. Vaccine 29: 5368–5378.
29. **Mora JR, et al.** 2006. Generation of gut-homing IgA-secreting B cells by intestinal dendritic cells. Science 314:1157–1160.
30. **Muramatsu M, et al.** 1999. Specific expression of activation-induced cytidine deaminase (AID), a novel member of the RNS-editing deaminase family in germinal center B cells. J. Biol. Chem. 274:18470–18476.
31. **Nguyen HH, et al.** 1999. Heterosubtypic immunity to lethal influenza A virus infection is associated with virus-specific CD8+ cytotoxic T lymphocyte responses induced in mucosa-associated tissues. Virology 254: 50–60.
32. **Nguyen HH, van Ginkel FW, Vu HL, McGhee JR, Mestecky J.** 2001. Heterosubtypic immunity to influenza A virus infection requires B cells but not CD8+ cytotoxic T lymphocytes. J. Infect. Dis. 183:368–376.
33. **Nishino M, et al.** 2009. Influenza vaccine with Surfacten, a modified pulmonary surfactant, induces systemic and mucosal immune responses without side effects in minipigs. Vaccine 27:5620–5627.
34. **Okumura Y, et al.** 2006. Serase-1B, a new splice variant of polyserase-1/TMPRSS9, activates urokinase-type plasminogen activator and proteolytic activation is negatively regulated by glycosaminoglycans. Biochem. J. 400:551–561.
35. **Pan H-Y, et al.** 2011. Up-regulation of ectopic trypsins in the myocardium by influenza A virus infection triggers acute myocarditis. Cardiovasc. Res. 89:595–603.
36. **Sato K, et al.** 1998. Therapeutic effect of erythromycin of influenza virus-induced lung injury in mice. Am. J. Respir. Crit. Care Med. 157:853–857.
37. **Sawabuchi T, et al.** 2009. Boost of mucosal secretory immunoglobulin A response by clarithromycin in pediatric influenza. Respirology 14: 1173–1179.
38. **Shikina T, et al.** 2004. IgA class switch occurs in the organized nasopharynx- and gut-associated lymphoid tissue, but not in the diffuse lamina propria of airways and gut. J. Immunol. 172:6259–6264.
39. **Takahashi E, et al.** 2010. Attenuation of inducible respiratory immune